Available online at www.sciencedirect.com
ScienceDirect
Journal of Volcanology and Geothermal Research 164 (2007) 127–141
Journal of volcanology and geothermal research
www.elsevier.com/locate/jvolgeores

Vent geometry and eruption conditions of the mixed rhyolite–basalt Námshraun lava flow, Iceland

Lionel Wilson [a,b,*], Sarah A. Fagents [b], Linda E. Robshaw [a], Evelyn D. Scott [a]

[a] *Environmental Science Department, Lancaster University, Lancaster LA1 4YQ, UK*
[b] *Hawai'i Institute of Geophysics and Planetology, University of Hawai'i at Manoa, 1680 East-West Road, Honolulu HI 96822, USA*

Received 13 October 2006; received in revised form 18 April 2007; accepted 21 April 2007
Available online 10 May 2007

Abstract

We describe the morphology and circumstances of eruption of the mixed rhyolite–basalt lava flow Námshraun in the Torfajökull–Veiðivötn area of central Iceland. The unusual location and exposure of the elongate fissure vent permits its length along strike (a total of ~275 m) and the width of the dyke feeding it (up to ~10 m) to be estimated in the field. Using analyses of the heat losses during the rise of the mixed magma through the shallow part of its conduit system, we are able to refine the absolute minimum dyke width estimate to ~1.5 m. The lengths of the two main lava flow lobes, assuming that their advance was cooling-limited, imply that the volume effusion rate of the lava varied between ~2.7 and ~1.5 $m^3\ s^{-1}$ as different parts of the fissure became active. Prior to its emergence at the surface the magma had at most a small yield strength (probably significantly less than ~3000–4000 Pa) and a near-Newtonian viscosity in the range $\sim 1\times10^4$ to $\sim 5\times10^6$ Pa s. After its eruption, the lava formed flows with marginal levées whose sizes imply a yield strength just less than 30 kPa. The lava in the central channels between the levées can be modeled either as a Newtonian fluid with a viscosity of between 3×10^7 and 6×10^7 Pa s or as a Bingham plastic. Estimates of the plastic viscosity from the two main flow lobes ($<10^4$ to $\sim 6\times10^5$ and 1.2×10^7 to 1.8×10^7 Pa s) differ by a very large factor (at least 30) and are regarded as unreliable; however, they lead to a much smaller range of apparent viscosities, from $\sim 1.5\times10^7$ to $\sim 5.5\times10^7$ Pa s, values very similar to the viscosities found when the rheology is assumed to be Newtonian. If the field estimate of the dyke width is reliable, these results imply that the viscosity (and yield strength) of the magma averaged over the path from its source to the surface had increased by a factor close to 10 by the time that it emerged from the vent; alternatively the feeder dike may have been almost twice as wide during the eruption and relaxed to the presently exposed width as the eruption ended. The typical advance speeds of the two main flow lobes were less than 4 mm s^{-1} and their emplacement times were ~2.5 and ~5 days. The implications for the sizes of the conduits feeding other rhyolitic and mixed lavas in central Iceland are discussed.
© 2007 Elsevier B.V. All rights reserved.

Keywords: rhyolite; mixed lava flow; rheology; Iceland; eruption rate

1. Introduction

Chemically composite volcanic intrusions have been described from the British Tertiary Volcanic Province and from Iceland (Blake et al., 1965; Walker and Skelhorn, 1966; Yoder, 1973). In eastern Iceland, some of these intrusions connect upward into composite lava flows (Gibson and Walker, 1963). In the vicinity of the lake Frostastaðavatn in the Landmannalaugar area of central-southern Iceland, several post-glacial mixed rhyolite–basalt lava flows are present (Walker, 1966; Sigurdsson, 1970; Saemundsson, 1972; Grönvold,

* Corresponding author. Environmental Science Department, Lancaster University, Lancaster LA1 4YQ, UK.
E-mail address: I.wilson@lancaster.ac.uk (L. Wilson).

0377-0273/$ - see front matter © 2007 Elsevier B.V. All rights reserved.
doi:10.1016/j.jvolgeores.2007.04.005

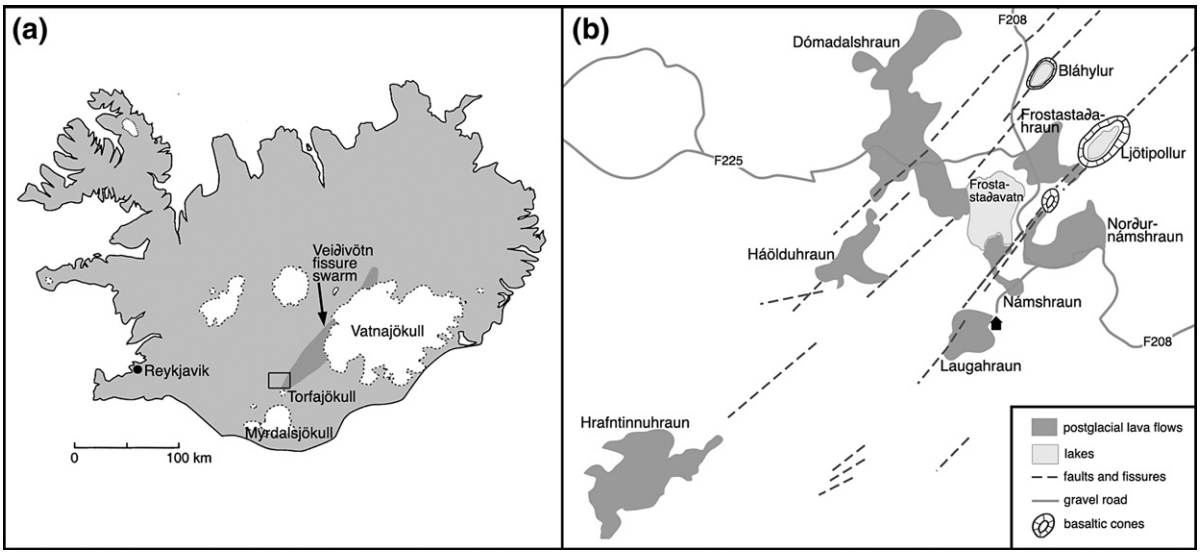


Fig. 1. (a) Map showing location of the Landmannalaugar area in south central Iceland. The Veiðivötn fissure swarm extends northeastwards under the Vatnajökull ice cap. Box shows area of detail in Fig. 1b. (b) Products of major post-glacial eruptions along the Veiðivötn fissure swarm. Norðurnámshraun and Frostastaðahraun are basaltic in composition, whereas the other flows are mixed basaltic–rhyolitic. Area shown in (b) is approximately 18×15 km.

1972; Walker, 1974; Jakobsson, 1979). These include the Dómadalshraun flow and the more recent Námshraun (sometimes referred to as Suðurnámshraun) and Laugahraun flows (Fig. 1). These mixed flows are interpreted to have formed as a result of lateral injection of southwestward-propagating tholeiitic dykes into the alkali-rhyolite magma chamber of the Torfajökull central volcano (Jakobsson, 1979).

Within the last ~1900 years, three such eruptions have taken place along the Veiðivötn fissure swarm (Fig. 1). The Dómadalshraun lava and Hnausar crater row were erupted in 150 AD, followed by the Hraftinnuhraun lava and the Vatnaöldur and Hnausapollur (also called Bláhylur) tholeiitic tephras in 900 AD (Larsen, 1984). A more recent lateral tholeiite injection event (1480 AD; Larsen, 1984) into the same chamber is interpreted (Jakobsson, 1979) to have produced the Veiðivötn lava, the Svartikrokur and Ljötipollur tephras, and the lava flows Norðurnámshraun (basalt), Námshraun (the mixed rhyolite studied here) and Laugahraun (a slightly mixed rhyolite). Similar lateral injection processes have been invoked to explain fissure eruptions at Krafla (Björnsson et al., 1977; Einarsson and Brandsdóttir, 1980), Sveinagjá (Sigurdsson and Sparks, 1978a), Eldgjá and Lakagigar (Sigurdsson and Sparks, 1978b). However, the assumption that these latter two fissure eruptions were fed by laterally propagating magma has been questioned by Thorðarson and Self (1993) who prefer a geometry involving vertical rise of mafic magma from shallow partial melting zones, and a model involving both horizontal and vertical magma propagation was postulated for Krafla by Björnsson (1985). In the present case we are only concerned with the final stages of vertical magma rise to the surface and

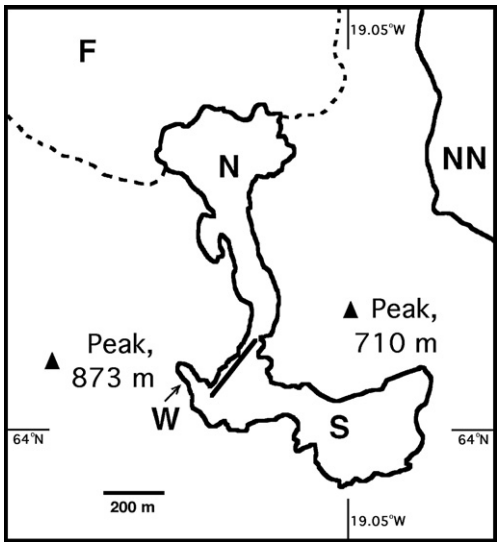


Fig. 2. Map of the study area. Labelled features are the northern (N), southern (S) and western (W) lobes of the Námshraun flow; the lake Frostastaðavatn (F) and the basaltic flow Norðurnámshraun (NN) are also shown. The solid line marks the location of the fissure vent system, situated on an irregular ridge joining the two marked peaks. Peak elevations are indicated; the lake level is ~570 m.

our analysis does not depend on knowing which direction of magma movement dominated at depth.

In general, no parts of the vents or feeder systems of the mixed lava flows in the Torfajökull area are exposed. This is due to the high viscosities of these magmas, which ensured that, as they erupted, lava piled up around the vent, completely hiding the geometry. However, one of these lavas, the Námshraun flow, was erupted under unusual geometrical circumstances. The vent is located on the crest of a ridge just south of Frostastaðavatn, and the steep slopes in the immediate vicinity of the vent (Fig. 2) permit its size and shape to be closely constrained. In this paper we describe the flow geometry and use theoretical models of the eruption process to place constraints on the effusion rate and rheology of the magma. These results are then used to draw inferences about the ranges of conditions that might be expected in future eruptions of this kind, many of which have occurred in south-central Iceland.

2. Morphology of the Námshraun flow

The Námshraun lava (Fig. 2) is located at 64° 01′ N, 19° 04′ W. It is of mixed rhyolite–basalt composition, with basalt inclusions on the sub-decimetre scale. The magma is dominated in terms of volume by the rhyolite component. The presence of the basalt inclusions may have increased the temperature of the magma and hence influenced its rheology indirectly, but it is the rhyolite component that forms the continuous liquid phase and dominates the bulk rheology. The vent for the Námshraun lava is a fissure system located near the crest of a ridge just south of Frostastaðavatn and it has two main flow lobes, one extending to the north (Figs. 2, 3) from the eastern part of the fissure system and the other to the south from the central part of the system (Fig. 2). A third, much smaller lobe extended towards the north-west, west and south-west from the western end of the fissure system (Fig. 2) and we refer to this as the western lobe. Immediately before the mixed lava eruption, the eastern vent appears to have given rise to a small basaltic eruption that built up a low spatter cone. When the much more viscous rhyolite–basalt magma emerged through the vent (Fig. 4) it formed a low spine that overtopped the basalt spatter-covered ridge to the north-east, feeding the flow lobe which traveled to the north.

Because the mixed rhyolite–basalt flow lobes set off almost immediately down very steep slopes, there was very little accumulation of lava around the vents. Also, the presence of the basaltic spatter helps to define the location of the eastern fissure vent segment particularly well. Based on assessment in the field (Fig. 4), we estimate the average width of the eastern part of the fissure to be an absolute minimum of ~1 m, more likely at least ~3 m, and a maximum of ~10 m. The eastern segment has a length along strike of ~65 m and the central segment is ~110 m long. The western segment is ~100 m long. The lengths of the mixed rhyolite–basalt flow lobes along their centre lines as deduced from Fig. 2 are ~790 m for the northern lobe and ~165 m for the western lobe. The total length of the southern lobe is ~870 m; however, due to a change in slope, we treat this as two distinct lengths of ~390 m for the upper portion and ~480 m for the lower.

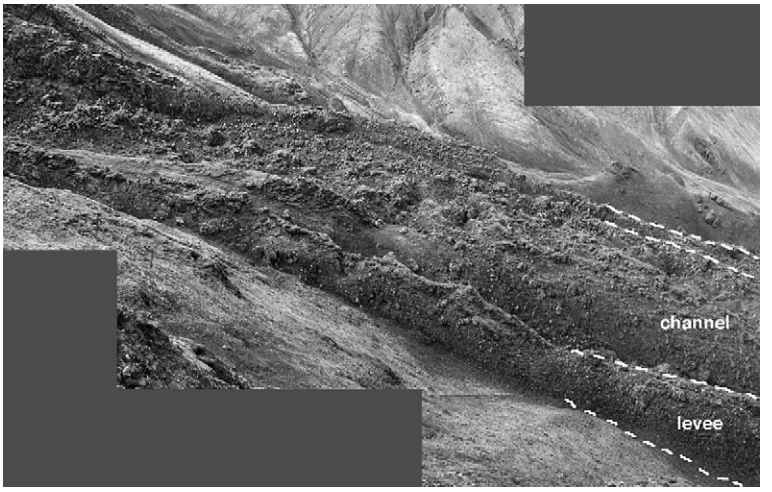


Fig. 3. View looking west across the channel of the north lobe of the Námshraun flow. The flow levées (partly picked out by white dashed lines) are clearly visible as narrow channel walls standing higher than the channel fill. The channel width in the central portion of the photograph is approximately 70 m. Photograph by S.A. Fagents.

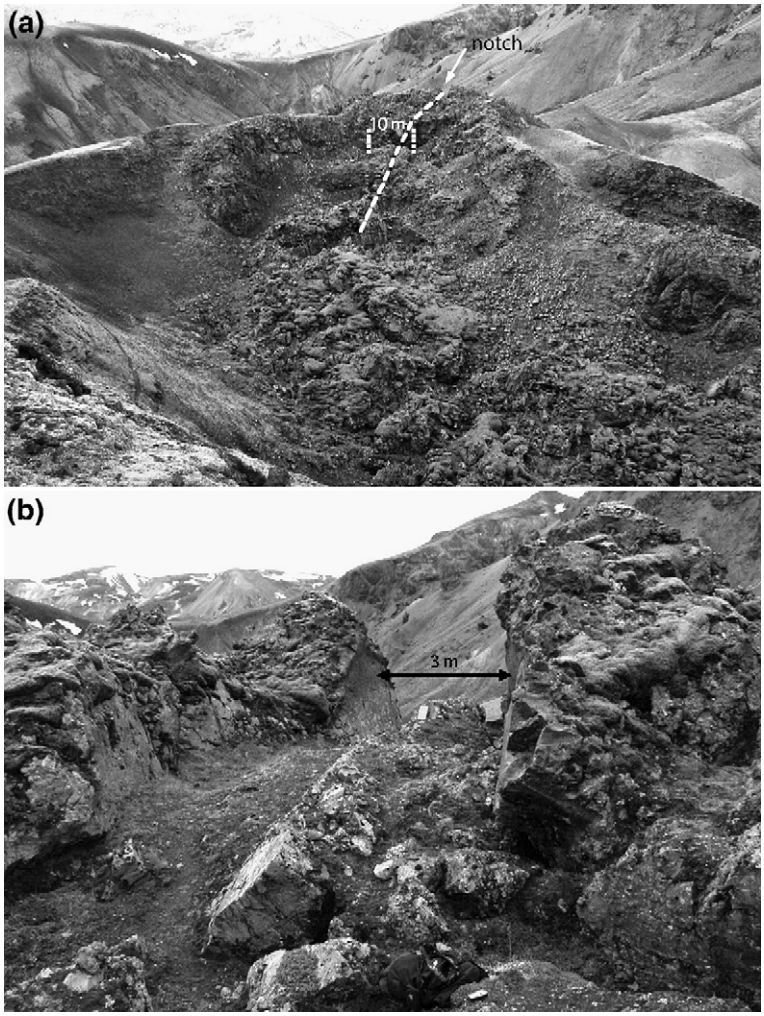


Fig. 4. The vent area of the Námshraun flow. (a) View into the vent area of the northern lobe from the basaltic spatter collar to the east of flow lobe. The surface manifestation of the fissure is highlighted by the dashed line, and the inferred maximum vent width is indicated by the two vertical dashed lines marking the edges of an outcrop of lava that appears to have been emplaced immediately above the fissure. The arrowed notch is the location of (b). (b) This notch at the crest of the ridge exposes the eruptive fissure. The smaller notebook rests on a 1 m wide protrusion of lava in a 3 m wide crevice. Photograph by S.A. Fxagents.

We focus here on the northern and southern flow lobes. The centre-line thicknesses, d_c (see Fig. 5 for definitions of flow geometry parameters), of these lobes on the steep slopes were estimated to be well in excess of 4 m and possibly up to 10 m; however, they were certainly less than 15 m, the value reached where the distal part of the

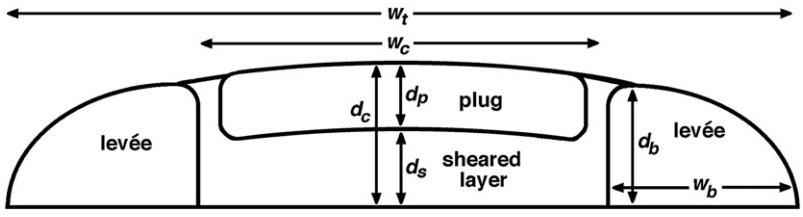


Fig. 5. Idealized cross-section of a Bingham plastic lava flow. Stationary levées of width w_b and maximum thickness d_b constrain lava to flow in a channel of width w_c. The total width of the flow, w_t, equals (w_c+2w_b). The shear stress in the upper part of the flowing lava is too small to cause shearing to occur, so the lava flows as an undeformed plug of thickness d_p. This rides on a layer of shearing lava of thickness d_s, and the total of these two thicknesses is the centre-line depth of the flow, d_c.

south flow moved onto almost flat ground. The plan-view areas of the northern and southern flow lobes were estimated from Fig. 2 as 1.3×10^5 m^2 and 1.6×10^5 m^2, respectively. Using an average thickness of ~10 m the total volume is $\sim3\times10^6$ m^3. The geometry of the northern flow lobe is fairly uniform where it descends the steepest parts of its path, and we estimate the average central channel width, w_c, here to be ~42±5 m and the average total width of the flow, w_t, to be ~70 m (Fig. 3). The southern lobe varies more along its length, with central channel widths in the upper, proximal section varying from ~32 m to ~107 m (±~10 m in each case), and in the lower, distal section from ~92±10 to ~152± 10 m, before the flow spreads out onto almost flat ground. Corresponding total flow widths average 88 m in the upper part and ~140 m in the lower part of the southern flow lobe. The average levée widths are 14±3 for the northern lobe and 9±6 m for the southern lobe. The average slopes of the flows are ~9° for the northern lobe, ~19° for the upper section of the southern lobe and ~3° for the lower southern lobe section.

3. Analysis of subsurface eruption dynamics

Let the volume eruption rate through the elongate fissure vent be F (see Table 1 for list of variables and symbols). F is related to the average magma rise speed, V, the width of the underlying dyke (assumed to be equal to the vent width), W, and the total active vent length along strike, L, by

$$F = WLV \tag{1}$$

The rise speed of a magma moving at a constant rate through a conduit connecting its source reservoir to the surface vent is controlled by the balance between wall friction and the spatial pressure gradient, dP/dz, driving the motion. The wall friction is a function of the rheology of the magma and the geometry of the conduit. Although there is considerable discussion as to the nature of the rheological properties of high-silica magmas in their source zones and feeder conduits (Pinkerton and Stevenson, 1992; Lejeune and Richet, 1995; Petford and Koenders, 1998; Bagdassarov and Dorfman, 1998) it seems possible that, as they approach the surface and are erupted, such magmas may undergo sufficient marginal cooling to cause them to behave at least approximately as Bingham plastics. Their motion is then characterized by a plastic viscosity, μ, and a yield strength, τ_y, which are related via

$$\varepsilon = \frac{1}{\mu}\left\{\begin{array}{ll} 0, & \tau_a \le \tau_y \\ (\tau_a - \tau_y), & \tau_a \ge \tau_y \end{array}\right\} \tag{2}$$

where ε is the strain rate and τ_a is the applied stress. The Bingham plastic approximation to the rheology of lava flowing in open channels and tubes has been used by numerous authors, e.g. Hulme (1974), Tallarico and Dragoni (2000), Dragoni et al. (1995), Tallarico et al. (2006). A lengthy derivation of the velocity profile in the fluid rising through an infinitely long fissure leads to the

Table 1
Definitions of variables used

Symbol	Definition	Units
D	Maximum distance that lava can flow	m^3 s^{-1}
F	Magma volume flux erupted through vent	m^3 s^{-1}
F_{min}	Minimum magma volume flux to avoid cooling	m^3 s^{-1}
G_{zc}	Critical value of Grätz number	Dimensionless
H	Depth of magma reservoir	m
He	Hedstrom number	Dimensionless
L	Surface fissure vent length along strike	m
Re	Reynolds number	Dimensionless
U	Mean flow speed of Newtonian lava in channel	m s^{-1}
V	Average rise speed of magma in conduit	m s^{-1}
V_{min}	Minimum rise speed of magma to avoid cooling	m s^{-1}
W	Surface fissure vent (and feeder dyke) width	m
W_p	Width of unsheared plug of mixed magma in dyke	m
d_b	Maximum thickness of lava flow levée	m
d_c	Maximum thickness of lava flow central channel	m
d_p	Thickness of plug of unsheared lava in central channel	m
d_s	Vertical depth of sheared lava beneath plug	m
dP/dz	Pressure gradient driving magma rise	Pa m^{-1}
$\hat{e}$	Average strain rate of lava beneath plug	s^{-1}
f	Friction factor	Dimensionless
g	Acceleration due to gravity	m s^{-2}
h_r	Hydraulic radius of lava flow	m
u_a	Average speed of lava in central channel of lava flow	m s^{-1}
u_p	Speed of unsheared plug of lava in flow channel	m s^{-1}
w_b	Width of lava flow levée	m
w_c	Width of central channel of lava flow	m
w_t	Total width of lava flow	m
ε	Mean strain rate of magma	s^{-1}
κ	Thermal diffusivity of lava	m^2 s^{-1}
μ	Plastic viscosity of magma in dyke	Pa s
μ_l	Plastic viscosity of lava in flow	Pa s
μ_{max}	Maximum allowed plastic viscosity of lava in flow	Pa s
μ_N	Newtonian viscosity of lava in flow	Pa s
ρ_b	Bulk density of magma	kg m^{-3}
ρ_c	Bulk density of country rocks	kg m^{-3}
τ_a	Shear stress applied to magma	Pa
τ_y	Yield strength of magma in dyke	Pa
τ_l	Yield strength of magma in levée	Pa

standard result (e.g., Skelland, 1967) that all of the shearing takes place in a zone extending inwards from the wall of the fissure to the edge of a central plug of unsheared fluid, the plug having a width W_p given by

$$W_p = \frac{2\tau_y}{dP/dz}, \quad (3)$$

where dP/dz is the absolute value of the pressure gradient in the z-direction driving the motion. We note that in a fissure of finite length the flow pattern is more complex, with unsheared stagnant plugs present at the corners of the fissure; this geometry has been treated by Tallarico and Dragoni (2000). In our simpler geometry the mean magma rise velocity, V, in the fissure is given by

$$V = \left(\frac{W}{f\rho_b}\frac{dP}{dz}\right)^{1/2} \quad (4)$$

where ρ_b is the bulk density of the magma. Here, f is a dimensionless friction factor which, when the fluid moves in a laminar fashion (an assumption which we shall justify retrospectively shortly), is given by the recursive relationship

$$f = \frac{24}{Re} + 3\frac{He}{Re^2} - \frac{4}{f^2}\left(\frac{He}{Re^2}\right)^3 \quad (5)$$

where Re is the Reynolds number, which for the fissure geometry is defined as

$$Re = \frac{2WV\rho_b}{\mu} \quad (6)$$

and He is the Hedstrom number, which for a fissure is

$$He = \frac{4\rho_b\tau_y W^2}{\mu^2} \quad (7)$$

Eqs. (4) and (5) explicitly assume that the fissure is much longer than it is wide, a good approximation in the present case.

If the expressions for Re and He given by Eqs. (6) and (7) are substituted into Eq. (5), and Eqs. (3) and (4) are used to substitute for τ_y and f, an equation can be constructed to give the mean magma rise speed V, which in turn can be substituted into Eq. (1) to give an expression for F:

$$F = \left(\frac{LdP/dz}{12\mu}\right)\left(W^3 - \frac{3}{2}W^2W_p + \frac{1}{2}W_p^3\right) \quad (8)$$

Earlier we quoted the field observations as showing W to be 1–10 m for all parts of the fissure vent system

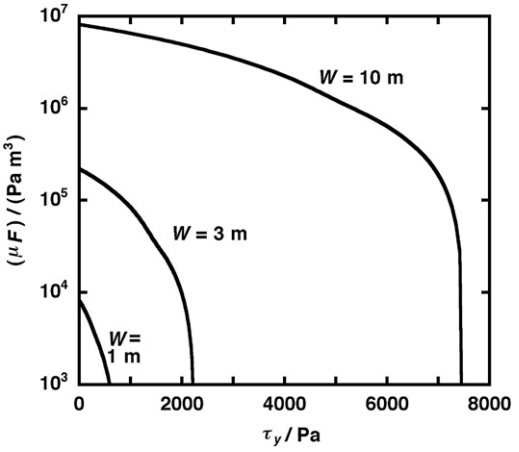


Fig. 6. Northern flow lobe: values of the product of the volume eruption rate F (in m^3 s^{-1}) and the plastic viscosity of the magma μ (in Pa s) for the maximum allowed range of values of the magma yield strength, τ_y (in Pa) in the dyke feeding the fissure vent, evaluated for dyke widths W of 1, 3 and 10 m. As τ_y goes to zero, μ becomes equal to the Newtonian viscosity of the magma.

and L to be ~110 m for the part of the vent feeding the southern flow lobe and ~65 m for the part of the vent feeding the northern lobe. We now estimate dP/dz by noting that the magma must have been driven to the surface either by its buoyancy relative to the surrounding rocks or by an excess pressure in its source region (or by both). Excess pressures in magma reservoirs are commonly of order a few MPa (Parfitt, 1991) and petrologic analyses (Gunnarsson et al., 1998) and seismic and magnetotelluric data (Zverev et al., 1980; Beblo et al., 1983; Eysteinsson and Hermance, 1985) suggest that rhyolitic magma reservoirs in this part of Iceland are at depths H of ~7–8 km. Thus, if an excess pressure is the cause of the eruption, the average value of dP/dz over the length of the magma pathway will be ~500 Pa m^{-1}. If buoyancy is the driving mechanism dP/dz will be given by $(g[\rho_c - \rho_b])$ where g is the acceleration due to gravity, ~9.8 m s^{-2}, and ρ_c is the density of the solid country rocks through which the magma of density ρ_b is ascending. The density of liquid rhyolite is about 2200 kg m^{-3} (Carmichael, 1989) and the density of the shallow crust in largely basaltic provinces such as Iceland is ~2300 kg m^{-3} (Gudmundsson, 1987), so that $(g[\rho_c - \rho_b])$ will be ~1000 Pa m^{-1}. Noting that both buoyancy and an excess pressure are likely to contribute, we adopt 1500 Pa m^{-1} as a plausible value for the total pressure gradient.

We obtain a family of possible eruption scenarios by choosing a range of values of τ_y and for each values of τ_y solving Eq. (8) for the product (μF). Possible values of τ_y range from zero to a maximum value that corresponds to

the central plug filling the fissure, given by Eq. (3) as $[(W\mathrm{d}P/\mathrm{d}z)/2]$. With $\mathrm{d}P/\mathrm{d}z = 1500$ Pa m^{-1} and $W = 1$ m, the maximum value of τ_y is 750 Pa; with $W = 3$ m it is 2250 Pa and with $W = 10$ m it is 7500 Pa. Figs. 6 and 7 show, for the northern and southern lobes, respectively, the implied values of $(\dot{\mu}F)$ for the allowed ranges of τ_y when W is 1, 3 and 10 m. It is clear that, since a significant eruption did take place, τ_y must have been significantly less than ~3000–4000 Pa even if the fissure width is at the upper end of the range we consider plausible from the field evidence, ~10 m, and is likely to have been considerably less. It could, of course, have been zero, in which case $\dot{\mu}$ becomes the Newtonian viscosity of the magma. Figs. 6 and 7 also imply that the product of the viscosity $\dot{\mu}$ and the volume flux F lies between about 8×10^3 and 8×10^6 Pa m^3 for the northern lobe and between about 1.3×10^4 and 1.3×10^7 Pa m^3 for the southern lobe. We now develop further constraints on $\dot{\mu}$ and F.

4. Constraints on magma effusion rate, F

Pinkerton and Wilson (1994) developed a model for the influence of cooling on the advance of lava flows. It was found that the maximum distance D that a flow could travel was related to the average lava flow speed during most of the advance of the flow, u, by

$$D = \frac{uh_r^2}{\kappa G_{zc}} \tag{9}$$

where h_r is the hydraulic radius of the flow, κ is the thermal diffusivity of the magma (~7×10^{-7} m^2 s^{-1} for all magmas) and G_{zc} is a critical value, equal to ~300, of the dimensionless Grätz number, essentially the square of the ratio of the thickness of the flow and the distance to which a wave of cooling has penetrated the flow. h_r is the ratio of the cross sectional area of moving magma divided by the wetted perimeter and, for a channelized flow (see Fig. 5) of thickness d_c and channel width w_c, is given by

$$h_r = \frac{d_c w_c}{w_c + 2d_c} \tag{10}$$

The average flow speed u can be expressed in terms of the volume effusion rate F using its definition

$$F = ud_c w_c \tag{11}$$

and combining these expressions gives

$$F = \frac{D\kappa G_{zc}(w_c + 2d_c)^2}{d_c w_c} \tag{12}$$

Using the dimensions mentioned earlier, $w_c = 42$ m, $D = 790$ m for the northern lobe and $w_c = 66$ to 146 m (average 106 m), $D = 870$ m for the southern lobe, and adopting $d_c = 10$ m for each flow thickness, we find $F = 1.52$ m^3 s^{-1} for the northern lobe and $F = 2.74$ m^3 s^{-1} for the southern lobe.

These values should be regarded as lower limits, since they assume that the flow lobes ceased to advance as a result of cooling; if the eruption was volume limited, and stopped because the magma supply was exhausted, the flow lobes would have advanced to greater distances if the eruption had continued. However, we infer that the presence of the short western flow lobe provides evidence for the two main flow lobes produced in this eruption being cooling limited. A possible scenario to explain the distribution of the erupted materials is that the southern flow lobe was erupted first; when this lobe ceased moving due to cooling limitations, the fissure vent (and presumably the shallow part of the feeder dyke system) extended along strike to the east allowing the northern flow lobe to be erupted. The volume eruption rate for this lobe was a little less than for the first lobe due to the reduction in driving pressure caused by the removal of magma from the source reservoir. When this lobe in turn ceased moving due to cooling, the fissure extended again, this time to the west, to allow the third lobe to begin to form. However, before this lobe reached its maximum potential distance the magma supply was exhausted and the eruption ceased. This argument would imply that the values of F given above are realistic, rather than lower limit, estimates of the effusion rate.

Coupled with the results summarized in Figs. 6 and 7, these values of $F = 1.52$ and 2.74 m^3 s^{-1} for the northern

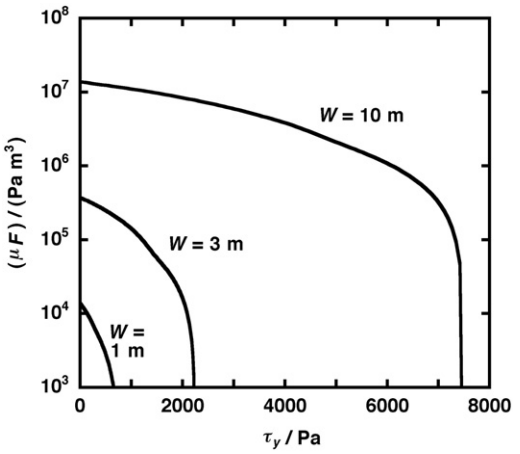


Fig. 7. Southern flow lobe properties: details as for Fig. 6.

and southern lobes imply that, as long as τ_y is not so large as to become the main control on the eruption process, $\dot{\mu}$ lies in the range $\sim 5.3\times10^3$ to $\sim 5.3\times10^6$ Pa s for the magma feeding the northern lobe and in the extremely similar range $\sim 5.0\times10^3$ to $\sim 5.0\times10^6$ Pa s for the magma feeding the southern lobe. If τ_y is very small these become estimates of the Newtonian viscosity of the magma. We now consider another way of constraining the eruption conditions.

5. Further constraints on magma viscosity, effusion rate and fissure width

The ability of magma to reach the surface from a reservoir at depth is limited by cooling through the dyke walls. Wilson and Head (1981) describe a treatment that defines the minimum speed (averaged across the fissure profile), V_{min}, at which magma with thermal diffusivity κ must rise to erupt with minimal cooling from a depth H. In the notation used here this is

$$V_{min} = \left(\frac{6.76\ \kappa H}{W^2}\right) \quad (13)$$

Using $H=\sim 7$–8 km as before and $\kappa = 7\times10^{-7}$ m^2 s^{-1}, we find $V_{min}=\sim 35$ mm s^{-1} when $W=1$ m, ~ 3.9 mm s^{-1} when $W=3$ m and ~ 0.36 mm s^{-1} when $W=10$ m.

For the northern flow lobe, these minimum rise speeds, together with the fissure length $L=65$ m, imply minimum volume fluxes of $F_{min}=WLV_{min}=2.31$ m^3 s^{-1} when $W=1$ m, $F_{min}=0.77$ m^3 s^{-1} when $W=3$ m and 0.23 m^3 s^{-1} when $W=10$ m. Coupled with the values of the product ($\dot{\mu}F$) shown in Fig. 6, these values of F_{min} imply maximum viscosities of $\dot{\mu}_{max}=\sim 3.5\times10^3$ Pa s when $W=1$ m, $\sim 2.9\times10^5$ Pa s when $W=3$ m and $\sim 3.5\times10^7$ Pa s when $W=10$ m. We now compare these values with the estimates of F and $\dot{\mu}$ from the previous Section. For $W=10$ m there are no inconsistencies: the derived value of $F=1.52$ m^3 s^{-1} is greater than the minimum value of $F_{min}=0.23$ m^3 s^{-1} and the maximum viscosity of $\dot{\mu}_{max}=\sim 3.5\times10^7$ Pa s is greater than the derived viscosity of 5.3×10^6 Pa s. Similarly for $W=3$ m there are no inconsistencies: the derived value of $F=1.52$ m^3 s^{-1} is greater than the minimum value of $F_{min}=0.77$ m^3 s^{-1} and the maximum viscosity of $\dot{\mu}_{max}=\sim 2.9\times10^5$ Pa s is greater than the derived viscosity of 1.4×10^5 Pa s. However for $W=1$ m there is complete inconsistency: the derived value of $F=1.52$ m^3 s^{-1} is less than the minimum value of $F_{min}=2.30$ m^3 s^{-1} and the maximum viscosity of $\dot{\mu}_{max}=\sim 3.5\times10^3$ Pa s is less than the derived viscosity of 5.3×10^3 Pa s. We take this to imply that the fissure width W cannot be as small as 1 m; interpolation between the above values shows that the derived values are just equal to the critical values when $W=\sim 1.6$ m, and we infer that this is the minimum possible value of W for the northern lobe. Adopting this value instead of the original field estimate of ~ 1 m changes the minimum magma viscosity estimate from 5.3×10^3 to 2.2×10^4 Pa s.

An exactly similar series of calculations can be carried out for the southern flow lobe. The minimum rise speeds of $V_{min}=35$ mm s^{-1} when $W=1$ m, 3.9 mm s^{-1} when $W=3$ m and 0.36 mm s^{-1} when $W=10$ m, together with the fissure length $L=110$ m, imply minimum volume fluxes of $F_{min}=WLV=3.85$ m^3 s^{-1} when $W=1$ m, $F_{min}=1.29$ m^3 s^{-1} when $W=3$ m and 0.39 m^3 s^{-1} when $W=10$ m. Coupled with the values of the product ($\dot{\mu}F$) shown in Fig. 7 these values of F_{min} imply maximum viscosities of $\dot{\mu}_{max}=\sim 3.6\times10^3$ Pa s when $W=1$ m, $\dot{\mu}_{max}=\sim 2.9\times10^5$ Pa s when $W=3$ m and $\dot{\mu}_{max}=\sim 3.5\times10^7$ Pa s when $W=10$ m. For both $W=10$ m and 3 m there is again no inconsistency: the derived values of F are greater than the minimum values F_{min} and the maximum viscosities are greater than the derived viscosities. However, as for the northern lobe, for $W=1$ m there is complete inconsistency: the derived value of $F=2.74$ m^3 s^{-1} is less than the minimum value of $F_{min}=3.85$ m^3 s^{-1} and the maximum viscosity of $\dot{\mu}_{max}=\sim 3.6\times10^3$ Pa s is less than the derived viscosity of 5.0×10^3 Pa s. Interpolation shows that the implied minimum possible value of W for the southern lobe is ~ 1.4 m. Again adopting this value instead of the original field estimate of ~ 1 m changes the minimum magma viscosity estimate from 5.0×10^3 to 1.1×10^4 Pa s.

6. Summary of pre-eruption magma properties

The analysis so far has been directed at estimating the properties of the magma rising toward the vent and the geometry of the dyke and vent system through which it erupted. Whereas field observations suggested that the width W of the feeder dyke probably lay in the range 1–10 m for the entire vent system, constraints on the cooling of the magma during its rise to the surface have refined this slightly to W being at least 1.6 m for the part of the vent feeding the northern lobe and 1.4 m for the part feeding the southern lobe. These values imply an upper limit on τ_y, the magma yield strength, the value being ~ 3000–4000 Pa for the magma feeding both the northern and southern lobes. The best estimates of the effusion rates are $F=1.52$ m^3 s^{-1} for the northern lobe and 2.74 m^3 s^{-1} for the southern lobe; combined with the active fissure lengths of 65 m and 110 m, respectively, they imply very similar effusion rates per unit length along strike of the

dyke of 0.023 and 0.025 $m^3\ s^{-1}\ m^{-1}$. Finally, combining the effusion rate estimates and the allowed ranges of fissure widths with the information in Figs. 6 and 7, as long as the yield strength is small the best estimates of the pre-eruption (Newtonian) magma viscosity are 2.2×10^4 to 5.3×10^6 Pa s for the magma feeding the northern lobe and 1.1×10^4 to 5.0×10^6 Pa s for that feeding the southern lobe.

7. Analysis of surface lava flow dynamics

7.1. General comments

When magma emerges at a surface vent to form a lava flow it is exposed to a significantly different cooling and deformation environment from that in the feeder dyke. Enhanced cooling, in particular, is likely to result in an increase in the viscosity and yield strength of the melt. Furthermore, if the lava flow develops a channel–levée structure, as was the case for the proximal parts of the northern and southern lobes of the Námshraun flow, the levées are generated from lava that has traveled to the flow front and been displaced laterally to make way for lava advancing down the central channel (Sparks et al., 1976). Thus the levée material at any given distance from the vent has been subjected to greater cooling than the central channel material, the difference in cooling time increasing as the eruption continues. This suggests that there is no reason to expect the materials in the levées and the central channel to have the same rheological properties.

7.2. Levée morphology

Hulme (1974) formulated relationships defining the morphology of a lava flow in terms of the lava bulk density, the acceleration due to gravity, the slope, α, of the ground on which the flow is moving, and the rheological properties of the lava, assuming all of the lava in the channel and levées to have the same Bingham plastic rheology. He postulated that lava flows consist of a central channel in which lava motion takes place between two banks or levées; the levées remain stationary once they have been emplaced because the shear stress at their bases is not enough to overcome the yield strength of the lava. The width, w_b, and maximum thickness, d_b, of each levée (Fig. 5) are then given by

$$w_b = \frac{\tau_l}{2\rho_b g \sin^2\alpha} \tag{14}$$

and

$$d_b = \frac{\tau_l}{\rho_b g \sin\alpha} \tag{15}$$

where τ_l is the yield strength of the levée material. These relationships apply at the time that a flow unit is being emplaced; naturally, continued cooling is likely to increase the yield strength of the levée material after it has been emplaced.

We consider Eqs. (14) and (15) to be a reasonable way to model the levées of a channelized flow, so that in principle τ_l can be estimated from measurements of w_b and α using Eq. (14) and/or d_b and α using Eq. (15). Fig. 8 shows the variations of w_b and d_b predicted by these equations as a function of τ_l. Recalling the estimates of w_b and d_b derived from field measurements and image analysis in Section 2, for the northern lobe ($w_b=\sim14$ m, $d_b=\sim4$–10 m) a reasonable fit is seen for $\tau_l=\sim1.5\times10^4$ Pa. For the upper part of the southern lobe ($w_b=\sim9$ m, $d_b=\sim4$–10 m), a reasonable fit exists for $\tau_l=\sim4\times10^4$ Pa. However, for the lower part of the southern lobe ($w_b=\sim9$ m, $d_b=\sim15$ m), no plausible value of τ_l can explain the observations. To be consistent with the 10–15 m thickness of the flow, its levées would have to be ~125 m wide, so that the total levée width would exceed the flow width. A major issue for this part of the southern flow lobe is the fact that it moved onto nearly flat ground and must have spread laterally as fast as it was advancing. Clearly, a model involving channelized flow is very inappropriate for the lava here.

Recalling that, in Hulme's (1974) model, the yield strength of central channel material is assumed to be equal to that of levée material, the centre-line thickness of a flow, d_c, is related to the total flow width, w_t, by

$$d_c = \left(\frac{\tau_l w_t}{\rho_b g}\right)^{1/2} \tag{16}$$

Thus τ_l can also be estimated from measurements of w_t and d_c using Eq. (16). In the present case, the overall morphologies of both the northern and southern flow units imply that the central channels drained to some extent on the steepest parts of the flows as the flow fronts were spreading onto flatter ground at the distal end of each flow unit. The currently observable central channel thicknesses are therefore significant underestimates of d_c as defined in Eq. (16). Using the value of $w_t=70$ m found for the northern lobe in Section 2, together with a median estimate of $d_c=\sim10$ m, the result is $\tau_l=\sim3.1\times10^4$ Pa, about double the value found from the levée geometry. The corresponding calculation for the upper part of the southern lobe, using $w_t=88$ m from Section 2 and again $d_c=\sim10$ m, gives $\tau_l=\sim2.5\times10^4$ Pa, about 60% of the value implied by the levée geometry. The mean of the values of τ_l derived from levée depths (1.5×10^4 and 4×10^4) and channel

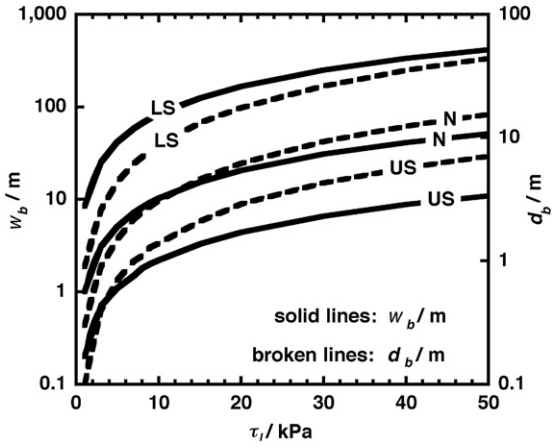


Fig. 8. For a range of assumed values of the yield strength of the levée material, τ_l, values are given for the implied width, w_b, and thickness, d_b, of the levées, for the northern lobe (N) and the upper (US) and lower (LS) parts of the southern lobe, of the Námshraun flow.

depths (3.1×10^4 and 2.5×10^4) is $\sim2.8\times10^4$ Pa. This value is ~8 times greater than the likely maximum pre-eruption yield strength estimates of 3000–4000 Pa given in Section 6.

The relatively poor correspondences between the values of τ_l derived from the levée depths and central channel depths cast doubt on the appropriateness of assuming that the central channel lava has the same properties as that in the levées. Nevertheless we proceed on that basis for the moment to explore the consequences.

7.3. Single rheology channel model

Hulme's (1974) model shows that the central channel width, w_c, can be related to the product of the volume flux and plastic viscosity μ_l of the lava in the channel. If w_c is less than the total width of the two levées, $(2w_b)$, the channel width is related to the other variables by

$$w_c = \left(\frac{24F\mu_l}{\tau_l \sin^2\alpha}\right)^{1/3} \tag{17}$$

If w_c is greater than the total width of the two levées, the relationship is

$$w_c = \left(\frac{\rho_b g\,(24F\mu_l)^4}{\tau_l^5 \sin^6\alpha}\right)^{1/11} \tag{18}$$

Note that the yield strength τ_l that appears in these equations is explicitly assumed to be equal to that of the lava in the levées. Eq. (17) and (18) are close approximations to Hulme's (1974) original single but much more complex polynomial (essentially of fifth order) expressing $(\mu_l F)$ in terms of the quantity $[w_c/(2w_b)]$. The approximations were introduced by Wilson and Head (1983) to make it possible to invert the equations and solve analytically for w_c. We employ these equations as follows. In the field it was not easy to identify the boundaries between the levées and central channels with great confidence, and the two most reliable quantities that can be measured for the flow lobes are the levée thicknesses d_b and the total flow width w_t. Using the definition of w_t,

$$w_t = w_c + 2w_b \tag{19}$$

Eqs. (14), (15), (19) and either (17) (when $w_c<2w_b$) or (18) (when $w_c>2w_b$) can be combined to yield

$$\mu_l = \left(\frac{\rho_b g d_b^{5/4}}{24F}\right)(w_t \sin\alpha - d_b)^{11/4}\ ,\ w_c > 2w_b \tag{20a}$$

$$\mu_l = \left(\frac{\rho_b g d_b}{24F}\right)(w_t \sin\alpha - d_b)^3\ \ ,\ w_c < 2w_b \tag{20b}$$

Average values of w_t were measured as ~70 m for the northern lobe, and ~88 and 140 m for the upper and lower parts, respectively, of the southern lobe. The corresponding slopes are ~9° for the northern lobe, ~19° for the upper section of the southern lobe and ~3° for the lower southern lobe section. Section 4 showed that $F=1.52$ m^3 s^{-1} for the northern lobe and $F=2.74$ m^3 s^{-1} for the southern lobe. Using these values, Fig. 9 shows how μ_l varies with d_b, taking into account that the maximum thicknesses of the

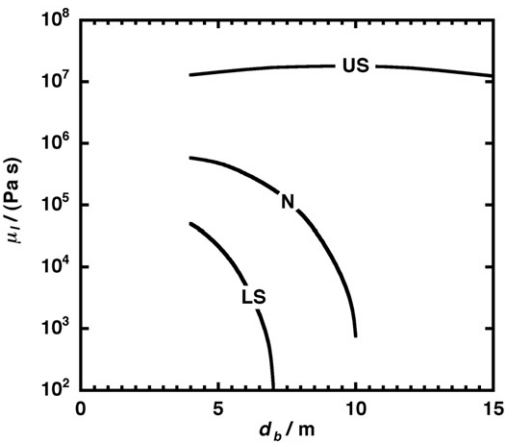


Fig. 9. Values of the implied plastic viscosity, μ_l, of lava in the central channels of the Námshraun flow lobes as a function of the levée thickness d_b when the same Bingham plastic rheology is assumed for the central channel and the levées.

Table 2
For a series of assumed thicknesses d_p of the plug on the surface of the lava treated as a Bingham plastic, values are given for the depth of the layer within which shearing is taking place d_s, the ratio of the average lava speed to the speed of the plug u_a/u_p, the plug speed u_p, the mean strain rate of the lava $\dot{e}$, the yield strength of the lava τ_y, its plastic viscosity $\dot{\mu}_l$, the average shear stress applied to the lava τ, and the resulting apparent viscosity of the lava μ_a

d_p (m)	d_s (m)	u_a/u_p	u_p (mm s^{-1})	$\dot{e}$ (s^{-1})	τ_y (kPa)	$\dot{\mu}_l$ (Pa s)	τ (kPa)	$\dot{\mu}_a$ (Pa s)
(a) Northern lobe of the Námshraun flow:								
4	6	0.80	4.52	7.54×10^{-4}	12.9	5.76×10^{5}	13.4	1.77×10^{7}
5	5	0.83	4.34	8.69×10^{-4}	16.2	4.81×10^{5}	16.6	1.91×10^{7}
6	4	0.87	4.18	1.04×10^{-3}	19.4	3.24×10^{5}	19.7	1.89×10^{7}
7	3	0.90	4.02	1.34×10^{-3}	22.6	1.78×10^{5}	22.9	1.71×10^{7}
8	2	0.93	3.88	1.94×10^{-3}	25.9	7.42×10^{4}	26.0	1.34×10^{7}
9	1	0.97	3.74	3.74×10^{-3}	29.1	1.81×10^{4}	29.2	7.80×10^{6}
(b) Upper southern lobe of the Námshraun flow:								
4	6	0.80	4.89	8.15×10^{-4}	28.1	1.24×10^{7}	38.2	4.69×10^{7}
5	5	0.83	4.70	9.39×10^{-4}	35.1	1.47×10^{7}	48.9	5.20×10^{7}
6	4	0.87	4.52	1.13×10^{-3}	42.1	1.64×10^{7}	60.6	5.37×10^{7}
7	3	0.90	4.35	1.45×10^{-3}	49.1	1.75×10^{7}	74.5	5.14×10^{7}
8	2	0.93	4.19	2.10×10^{-3}	56.1	1.82×10^{7}	94.3	4.50×10^{7}
9	1	0.97	4.05	4.05×10^{-3}	63.1	1.84×10^{7}	137.6	3.40×10^{7}
(c) Lower southern lobe of the Námshraun flow:								
4	11	0.76	1.98	1.80×10^{-4}	4.54	5.05×10^{4}	4.55	2.53×10^{7}
5	10	0.78	1.92	1.92×10^{-4}	5.68	2.20×10^{4}	5.68	2.95×10^{7}
6	9	0.80	1.87	2.08×10^{-4}	6.82	5.12×10^{3}	6.82	3.28×10^{7}
7	8	0.82	1.82	2.28×10^{-4}	7.95	1.22×10^{2}	7.95	3.49×10^{7}

levées on the steepest slopes were estimated to be well in excess of 4 m but probably no more than 10 m and certainly less than 15 m. For the northern lobe, the implied values of $\dot{\mu}_l$ depend very strongly on the value assumed for d_b, and range from 5.8×10^5 to less than 10^4 Pa s. The values of $\dot{\mu}_l$ for the upper part of the southern lobe vary less, ranging from 1.2×10^7 to 1.8×10^7, but they are 50 to 200 times larger than those for the northern lobe.

This large discrepancy is another indicator that the single-rheology approach to modeling the flow lobes is inappropriate. However, for comparison with the next section, which treats the lava in the central channels of the flow lobes as Newtonian, we present the following illustration of the problems associated with interpreting lava flow motion in terms of rheology. Fig. 5 shows the cross-section of a channel in which a Bingham plastic lava is flowing. An unsheared plug of depth d_p rides at speed u_p on a layer of depth d_s in which all of the shearing takes place. The total flow thickness is $d_c=d_p+d_s$. The velocity profile within the sheared layer is parabolic, and a simple integral shows that the mean speed within the layer, u_s, is equal to (2/3) u_p. Thus the overall average speed of the lava in the channel is u_a where

$$u_a = \left(\frac{u_p d_p + \frac{2}{3}u_p d_s}{d_p + d_s}\right) = u_p\left(\frac{d_p + \frac{2}{3}d_s}{d_p + d_s}\right) \qquad (21)$$

which allows u_p to be determined from u_a. Then the average strain rate $\dot{e}$ within the shearing layer is the spatial average of (u/d) within the layer, readily shown to be (3/2) (u_p/d_s). Finally, from Eq. (2) the average shear stress applied to the lava is $\tau=(\tau_y+\dot{e}\dot{\mu}_l)$, and its apparent viscosity is $\dot{\mu}_a=\tau/\dot{e}=[(\tau_y/\dot{e})+\dot{\mu}_l]$.

Table 2 summarizes the relevant values of these quantities for each of the lobes. They are calculated using the following parameters: for the northern lobe $d_c=10$ m and $u_a=F/(w_c d_c)$ with, as before, $F=1.52$ m^3 s^{-1} and $w_c=42$ m, so that $u_a=3.62$ mm s^{-1}; for the upper part of the southern lobe $d_c=10$ m, $F=2.74$ m^3 s^{-1}, $w_c=70$ m, and $u_a=3.91$ mm s^{-1}; and for the lower part of the southern lobe $d_c=15$ m, $F=2.74$ m^3 s^{-1}, $w_c=122$ m, and $u_a=1.50$ mm s^{-1}. The values of $\dot{\mu}_l$ are calculated from Eqs. (20a) or (20b) and the values of τ_y are obtained from Eq. (15). Fig. 10 summarizes the key results from Table 2: the plug speeds u_p in part (a), the yield strengths τ_y in part (b), the plastic viscosities $\dot{\mu}_l$ in part (c) and the apparent viscosities $\dot{\mu}_a$ in part (d). Fig. 10(d) demonstrates that the apparent viscosities of the various parts of the lobes ($\sim1.5\times10^7$ Pa s for the northern lobe, $\sim4.7\times10^7$ Pa s for the upper part of the southern lobe and $\sim3.0\times10^7$ Pa s for its lower part) generally cluster much more closely than the plastic viscosities. The way in which the yield strength, plastic viscosity and apparent viscosity are related makes it clear that small changes in the stress

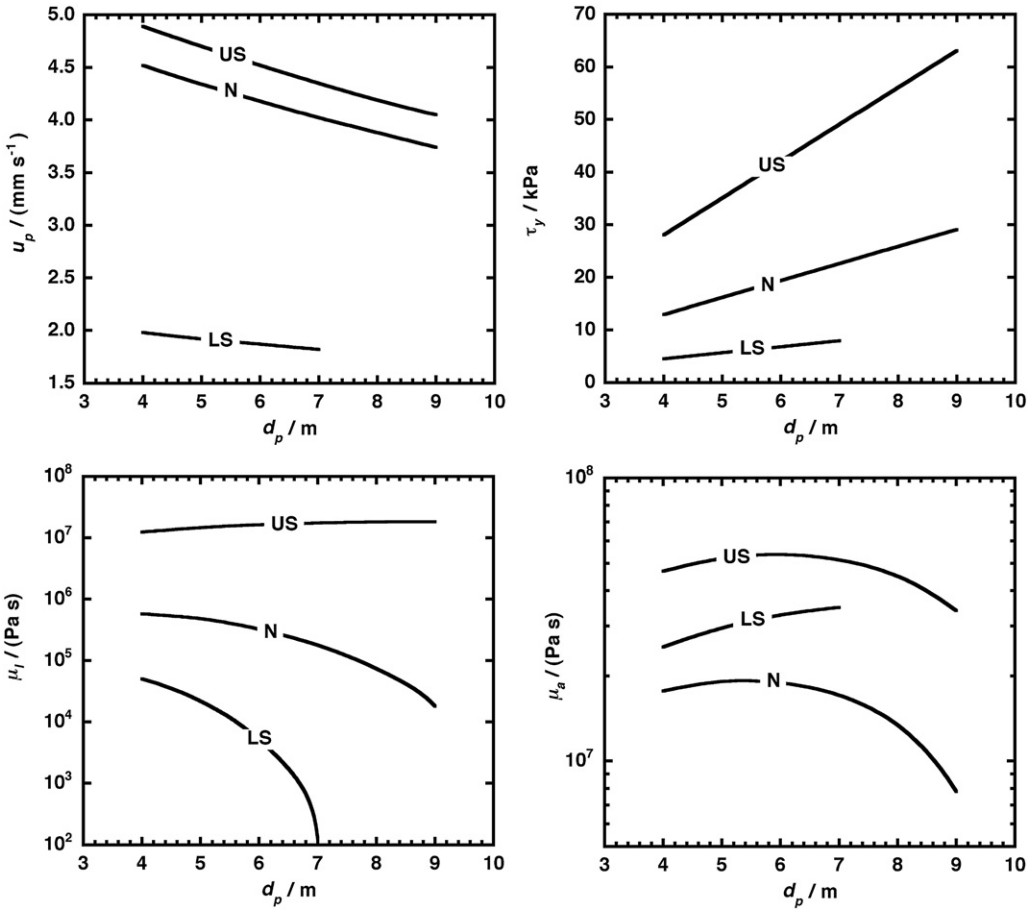


Fig. 10. For a series of assumed thicknesses d_p of the plug on the surface of the lava treated as a Bingham plastic, values are given for (a) the plug speed u_p, (b) the yield strength of the lava τ_y, (c) the plastic viscosity of the lava μ_l, and (d) the resulting apparent viscosity of the lava μ_a. The letter labels N, US and LS refer to the Northern and to the Upper Southern and Lower Southern lobes, respectively. See text and Table 2 for more details.

applied to the flow make large changes in its deformation rate and hence its apparent viscosity. Conversely, extremely accurate measurements of a flow's geometry and motion would be needed to obtain accurate measurements of its plastic viscosity.

7.4. Dual rheology model

We now assume, as argued in Section 7.1, that the formation of levées can be regarded as a flow-front process that has little connection with the properties of the lava in the central channel of a channelized flow. We therefore treat the lava in the central channels of both flow lobes as a Newtonian fluid. It is true that in Section 3 we allowed the possibility of the lava having a small pre-eruption yield strength of up to 3000–4000 Pa, which, it might be argued, would cause the lava in a central channel to exhibit plug-flow; but Eq. (15) shows that a yield strength of this order will lead to an unsheared plug thickness of only 0.8 m even on the steepest (19°) slope relevant here, and this is so much less than the ~10 m thickness of the flow lobes that it can be neglected. Assuming the motion is laminar, a flow of Newtonian fluid in a channel that is much wider than it is deep moves down a slope α at speed U given by

$$U = \left(\frac{\rho_b g d_c^2 \sin\alpha}{3\mu_N}\right) \tag{22}$$

where μ_N is the Newtonian viscosity and d_c is the flow depth. The volume flux, F, is equal to $(U d_c w_c)$ where w_c is the channel width, and combining this with Eq. (22) leads to

$$\mu_N = \left(\frac{\rho_b g w_c d_c^3 \sin\alpha}{3F}\right) \tag{23}$$

Inserting the appropriate values for the northern lobe, w_c=42 m, α=9°, F=1.52 m^3 s^{-1} and using d_c=10 m

yields $\mu_N = 3.1 \times 10^7$ Pa s. For the upper part of the southern lobe, $w_c = 70$ m, $\alpha = 19°$, $F = 2.74$ m^3 s^{-1} and again using $d_c = 10$ m yields $\mu_N = 6.0 \times 10^7$ Pa s. Earlier we expressed concern about using a channelized flow approximation for the lower part of the southern lobe, but if we do so we find that $w_c = 122$ m, $\alpha = 3°$, $F = 2.74$ m^3 s^{-1} and the field estimate of $d_c = 15$ m yield $\mu_N = 3.8 \times 10^7$ Pa s, similar to the value for the northern lobe. Although, taken together, these three estimates vary by a factor of two, they are very much more mutually consistent than the plastic viscosities derived from the single-rheology model. Also, perhaps not surprisingly, they are quite similar to the apparent viscosities obtained from the single-rheology model.

8. Discussion

The average of the Newtonian viscosities deduced in Section 7.4 for the northern and southern flow lobes, $\sim 4.3 \times 10^7$ Pa s, is ~ 10 times larger than the pre-eruption Newtonian viscosity estimate, $\sim 5 \times 10^6$ Pa s, from Section 6. The average of the yield strengths deduced for the flow lobes in Section 7.2, $\sim 2.8 \times 10^4$ Pa, is approximately 8 times greater than the maximum pre-eruption yield strength estimates of 3000–4000 Pa from Section 6. We have assumed uniform conditions in the feeder dyke, and so the pre-eruption values reflect an average of the properties of the magma during its rise from its source to the surface. It appears that a significant change in the rheology of the magma had occurred by the time it emerged through the vent. The only way to eliminate the requirement for this change is to force the pre-eruption magma properties to closely approximate the post-eruption values. Using the relationships in Section 5 to do this, we find that this could be done if the dyke were just slightly less than 20 m wide. This is a factor of 2 greater than our largest width estimate based on the observed morphology of the vent region, but it could possibly reflect significant relaxation of the dyke as the excess pressure in the magma source was removed by the eruption event.

9. Summary and comments

The two main lobes of the Námshraun mixed lava flow have a total volume of $\sim 3 \times 10^6$ m^3. The unusual location at the top of a ridge and the consequent good exposure of the elongate fissure vent permits its total length along strike (~ 275 m) and the width of the dyke feeding it (~ 10 m) to be estimated in the field. Consideration of heat losses during the rise of the magma through the feeder dyke requires the absolute minimum dyke width to be ~ 1.5 m, but the analyses of the dynamics suggest that the dyke may have had a greater (up to ~ 20 m) width while active, relaxing to the presently observed width as the eruption ended. The lengths of the two main lava flow lobes, given the field evidence that their advance was cooling-limited, imply that the volume effusion rate of the lava varied between ~ 2.7 and ~ 1.5 m^3 s^{-1}. The typical advance speeds of the two main flow lobes were less than 4 mm s^{-1} and their emplacement times were ~ 2.5 and ~ 5 days.

At depth the magma had at most a small yield strength (probably much less than 3000 Pa) and a near-Newtonian viscosity in the range $\sim 1 \times 10^4$ to $\sim 5 \times 10^6$ Pa s. On eruption, the lava formed flows with marginal levée sizes implying a yield strength near 30 kPa. The lava in the central channels between the levées can be modeled either as a Newtonian fluid with a viscosity of between 3×10^7 and 6×10^7 Pa s or as a Bingham plastic. Plastic viscosity estimates from the two main flow lobes ($< 10^4$ to $\sim 6 \times 10^5$ and 1.2×10^7 to 1.8×10^7 Pa s) cover a wide range and differ by a factor of at least 30, and are not regarded as reliable; however, they lead to a much narrower range of apparent viscosities, $\sim 1.5 \times 10^7$ to $\sim 5.5 \times 10^7$ Pa s, similar to the values found when Newtonian rheology is assumed. These results appear to imply that the viscosity and yield strength of the magma increased ~ 10-fold between its leaving its source and forming flows on the surface. This apparent change in properties can be eliminated if we assume that, over most of its vertical length, the feeder dyke was about a factor of 2 wider than what is implied by the observable surface fissure.

There are a number of other rhyolitic and mixed rhyolite–basalt lava flows in the Torfajökull area (Fig. 1b). These generally have flow lobe lengths comparable to those of Námshraun, though the largest, Dómadalshraun, has lobes with lengths 2–3 times greater and widths ~ 2 times greater than those of Námshraun. The multiple nature of Dómadalshraun's flow lobes suggests that they were cooling-limited, and so the application of Eq. (12) implies eruption rates ~ 5 times larger than those of the Námshraun lobes, say ~ 10 m^3 s^{-1}. Unfortunately, the vent for the Dómadalshraun flow is located at the top of a low rise, and the extent of lava accumulation around it is very great: a continuous mound measuring ~ 600 by 240 m is visible in aerial photographs. Clearly there is no possibility of estimating the vent size even as crudely as to within an order of magnitude. Thus we cannot tell if the greater effusion rate is the result of a wider feeder dyke or simply a greater horizontal dyke outcrop. If the difference

in effusion rate were attributed entirely to dyke width, however, Eq. (8) shows that, as long as the magma yield strength is not large, the volume flux is proportional to the cube of the dyke width, and so only a 70% increase in dyke width would be needed to cause a 5-fold increase in eruption rate. The implication seems to be that small (lengths up to a few kilometres) rhyolite-dominated lava flows do not commonly involve particularly wide vent systems, despite the high viscosity of such magmas. We note that many rhyolite vent size estimates in the literature (many tens to a few hundreds of metres) are derived from high magma discharge rates inferred during rhyolitic plinian eruptions, and probably give a false impression of the vent sizes involved in the production of small-volume rhyolite lava flows.

Acknowledgements

This work was supported in part by European Commission grant ENV4-CT96-0259. EDS also thanks the Open University for partial financial support from the Ian Gass Bursary. We are very grateful to Andrea Tallarico and an anonymous reviewer for comments that helped improve the presentation of the results. This is HIGP publication number 1487 and SOEST publication number 7110.

References

Bagdassarov, N., Dorfman, A., 1998. Granite rheology: magma flow and melt migration. J. Geol. Soc. (Lond.) 155, 863–872.

Beblo, M., Björnsson, A., Arnason, K., Stein, B., Wolfgram, P., 1983. Electrical-conductivity beneath Iceland — constraints imposed by magnetotelluric results on temperature, partial melt, crust-structure and mantle structure. Z. Geophys. 53 (1), 16–23.

Björnsson, A., 1985. Dynamics of crustal rifting in NE Iceland. J. Geophys. Res. 90, 10151–10162.

Björnsson, A., Saemundsson, K., Einarsson, P., Tryggvason, E., Grönvold, K., 1977. Current rifting episode in north Iceland. Nature 266, 318–323.

Blake, D.H., Elwell, R.W.D., Gibson, I.L., Skelhorn, R.R., Walker, G.P.L., 1965. Some relationships resulting from the intimate association of acid and basic magmas. Q. J. Geol. Soc. Lond. 121, 31–49.

Carmichael, R.S., 1989. Practical Handbook of Physical Properties of Rocks and Minerals. CRC Press, Boca Raton, FL. 741 pp.

Dragoni, M., Piombo, A., Tallarico, A., 1995. A model for the formation of lava tubes by roofing over a channel. J. Geophys. Res. 100, 8435–8447.

Einarsson, P., Brandsdóttir, B., 1980. Seismological evidence for lateral magma intrusion during the July 1978 deflation of the Krafla volcano in NE-Iceland. J. Geophys. 47, 160–165.

Eysteinsson, H., Hermance, J.F., 1985. Magnetotelluric measurements across the eastern neovolcanic zone in south Iceland. J. Geophys. Res. 90 (B12), 93–103.

Gibson, I.L., Walker, G.P.L., 1963. Some composite rhyolite–basalt lavas and related dykes in eastern Iceland. Proc. Geol. Assoc. 74, 301–318.

Grönvold, K., 1972. Structural and petrochemical studies in the Kerlingarfjöll region, central Iceland. D. Phil. thesis, Univ. of Oxford, 250 pp.

Gudmundsson, A., 1987. Lateral magma flow, caldera collapse, and a mechanism of large eruptions in Iceland. J. Volcanol. Geotherm. Res. 34, 65–78.

Gunnarsson, B., Marsh, B.D., Taylor, H.P., 1998. Generation of Icelandic rhyolites: silicic lavas from the Torfajokull central volcano. J. Volcanol. Geotherm. Res. 83 (1–2), 1–45.

Hulme, G., 1974. The interpretation of lava flow morphology. Geophys. J. R. Astron. Soc. 39, 361–383.

Jakobsson, S.P., 1979. Petrology of recent basalts of the Eastern Volcanic Zone, Iceland. Acta Nat. Isl. 26, 103 pp.

Larsen, G., 1984. Recent volcanic history of the Veiðivotn fissure swarm, southern Iceland — an approach to volcanic risk assessment. J. Volcanol. Geotherm. Res. 22 (1–2), 33–58.

Lejeune, A.M., Richet, P., 1995. Rheology of crystal-bearing silicate melts: an experimental study at high viscosities. J. Geophys. Res. 100, 4215–4229.

Parfitt, E.A., 1991. The role of rift zone storage in controlling the site and timing of eruptions and intrusions of Kilauea volcano, Hawaii. J. Geophys. Res. 96, 10101–10112.

Petford, N., Koenders, M.A., 1998. Granular flow and viscous fluctuations in low Bagnold number granitic magmas. J. Geol. Soc. (Lond.) 155, 873–881.

Pinkerton, H., Stevenson, R., 1992. Methods of determining the rheological properties of magmas at subsolidus temperatures. J. Volcanol. Geotherm. Res. 53, 47–66.

Pinkerton, H., Wilson, L., 1994. Factors controlling the lengths of channel-fed lava flows. Bull. Volcanol. 56, 108–120.

Saemundsson, K., 1972. Notes on the geology of the Torfajokull central volcano (in Icelandic with English summary). Náttúrufraedingurinn 42, 81–99.

Sigurdsson, H., 1970. The petrology and chemistry of the Setberg volcanic region and of intermediate and acid rocks of Iceland. PhD thesis, Univ. of Durham, 308 pp.

Sigurdsson, H., Sparks, R.S.J., 1978a. Rifting episode in north Iceland in 1874–1875 and the eruptions of Askja and Sveinagjá. Bull. Volcanol. 41, 149–167.

Sigurdsson, H., Sparks, R.S.J., 1978b. Lateral magma flow within rifted Icelandic crust. Nature 274, 126–130.

Skelland, A.H.P., 1967. Non-Newtonian Flow and Heat Transfer. John Wiley, New York. 469 pp.

Sparks, R.S.J., Pinkerton, H., Hulme, G., 1976. Classification and formation of lava levees on Mount Etna, Sicily. Geology 4 (5), 269–271.

Tallarico, A., Dragoni, M., 2000. A three-dimensional Bingham model for channeled lava flows. J. Geophys. Res. 105, 25969–25980.

Tallarico, A., Dragoni, M., Zito, G., 2006. Evaluation of lava effusion rate and viscosity from other flow parameters. J. Geophys. Res. 111, B11205. doi:10.1029/2005JB003762.

Thorðarson, T., Self, S., 1993. The Skaftár Fires (Laki) and Grímsvötn eruptions in 1783–1785. Bull. Volcanol. 55, 233–263.

Walker, G.P.L., 1966. Acid volcanic rocks in Iceland. Bull. Volcanol. 29, 375–406.

Walker, G.P.L., 1974. Eruptive mechanisms in Iceland. In: Kristjansson, L. (Ed.), Geodynamics of Iceland and the North Atlantic Area. Reidel Publ, Dordrecht, pp. 189–201.

Walker, G.P.L., Skelhorn, R.R., 1966. Some associations of basic and acid igneous rocks. Earth Sci. Rev. 2, 93–109.

Wilson, L., Head, J.W., 1981. Ascent and eruption of basaltic magma on the Earth and Moon. J. Geophys. Res. 86, 2971–3001.

Wilson, L., Head, J.W., 1983. A comparison of volcanic eruption processes on Earth, Moon, Mars, Io and Venus. Nature 302, 663–669.

Yoder, H.S., 1973. Contemporaneous basaltic and rhyolitic magmas. Am. Mineral. 58, 153–171.

Zverev, S.M., Litvinenko, I.V., Palmason, G., Yaroshevskaya, G.A., Osokin, N.N., 1980. Seismic crustal study of the axial rift-zone in southwest Iceland. Z. Geophys. 47 (1–3), 202–210.